

Thermodynamic Investigation of Carbon Deposition and Sulfur Evolution in Chemical Looping Combustion with Syngas

Baowen Wang,^{†,‡} Rong Yan,^{*,‡} Dong Ho Lee,[‡] David Tee Liang,[‡] Ying Zheng,[†]
Haibo Zhao,[†] and Chuguang Zheng[†]

State Key Laboratory of Coal Combustion, Huazhong University of Science and Technology, Wuhan 430074, P.R. China, and Institute of Environmental Science and Engineering, Nanyang Technological University, Innovation Center, Block 2, Unit 237, 18 Nanyang Drive, Singapore 637723

Received September 21, 2007. Revised Manuscript Received December 18, 2007

Chemical looping combustion (CLC) with syngas, a synthesized gas mixture of CO, H₂, CO₂, H₂O(g), N₂, and H₂S, was investigated using thermodynamic simulation, with focus on carbon deposition and sulfur evolution in CLC. Five metal oxides, such as NiO, CuO, Fe₂O₃, Mn₃O₄, and CoO, were selected as oxygen carriers for CLC application. Different influencing factors on the formation of carbon deposits were investigated, including pressure, fuel reactor (FR) temperature, oxygen excess number Φ (denoting the availability of lattice oxygen in the oxygen carrier to the fuel), and fuel gas composition. Higher temperature and larger oxygen excess number Φ inhibited the formation of carbon deposits while the pressurized condition caused the opposite. The increase of H₂O(g) and CO₂ fraction in syngas reduced carbon deposition while, in contrast, a larger H₂S occurrence in syngas led to more carbon deposits to be formed. A sensitivity analysis to the different factors revealed that carbon deposition was mainly determined by the FR temperature and the oxygen carriers provided while other factors played a minor role. In addition, the predominant C-bearing species and their distributions at different temperatures were thermodynamically investigated. At low FR temperature and oxygen-deficient condition (i.e., oxygen excess number $\Phi < 1$), the predominant carbon species as solid deposits were mainly elemental carbon or carbonates for NiO, CuO, Fe₂O₃, and CoO while MnC₂ and MnCO₃ were the main species for Mn₃O₄. In terms of the evolution of sulfur in CLC with syngas containing a basic composition of CO, N₂, H₂, and H₂S, the low pressure, high temperature, and adequate lattice oxygen would make more sulfur species form in the gas phase. After that, CO₂ and H₂O(g) were introduced into the syngas, and they were found to possibly serve as additional oxidizers to convert H₂S into SO₂. The oxidation function of CO₂ was slightly stronger than that of steam. Again, the evolution and distribution of various sulfur species was studied. For four metal oxides (NiO, Fe₂O₃, Mn₃O₄, and CoO), the most possible solid sulfur compounds were Ni₃S₂, Fe_{0.84}S, MnSO₄, and Co_{0.89}S, respectively. But for CuO, at $\Phi < 1$, Cu₂S was the main solid sulfur compound while at $\Phi > 1$ CuSO₄ and Cu₂SO₄ dominated.

1. Introduction

Public increasing concern over global warming and the severe problems related to climate change necessitate the control of CO₂ emission from fossil fuels, especially coal.¹ Currently, the major technologies for CO₂ abatement are classified into postcombustion, precombustion decarbonization, and oxy-fuel combustion technologies. However, all of these technologies generally require gas separation and therefore much energy consumption. Fundamentally different to them, chemical looping combustion (CLC), a novel method, addresses the CO₂ capture by completely avoiding any gas separation.² The CLC system is composed of two reactors, an air reactor (AR) and a fuel reactor (FR), as shown in Figure 1, where the air and fuel are never mixed together. In the FR, the fuel is oxidized with metal oxides M_xO_y instead of air in the normal combustion. At the

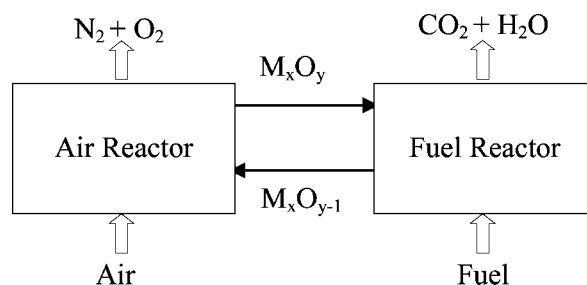


Figure 1. Scheme of CLC. M_xO_y/M_xO_{y-1} denotes the oxidized and reduced oxygen carriers, respectively.

full conversion of fuel, the exit gas stream from the FR mainly consists of CO₂ and steam. Pure CO₂ will be readily recovered by condensing the steam. The reduced metal oxide M_xO_{y-1} is then transferred from the FR to the AR, where it is reoxidized by air. Compared to the normal combustion, because CO₂ in CLC is not diluted with N₂ in the air, it can easily be separated without much energy consumption. Another two verified advantages for CLC are, first, to thoroughly eradicate the formation of NO_x, as a result of the introduction of fuel and air into different reactors and of the moderate AR operating

* To whom correspondence should be addressed. Telephone: (65)67943244. Fax: (65)67921291. E-mail: ryan@ntu.edu.sg.

[†] Huazhong University of Science and Technology.

[‡] Nanyang Technological University.

(1) IPCC Special Report on Carbon Dioxide Capture and Storage; Cambridge University Press: New York, 2005.

(2) Eide, L. I.; Anheden, M.; Lyngfelt, A.; Abanades, C.; Younes, M.; Clodic, D.; Bill, A. A.; Feron, P. H. M.; Rojey, A.; Giroudiere, F. Novel capture processes. *Oil Gas Sci. Technol.* **2005**, *60* (3), 497–508.

temperature,³ and, then, to improve the thermal efficiency of fuel combustion as a result of the lesser irreversibility of fuel oxidation.⁴ Therefore, using CLC can simultaneously solve energy and environmental problems.⁵

In CLC-related research, the oxygen carrier development and further optimization of their performances attract the most interest.^{6–9} Currently, the main oxygen carriers considered are Ni, Cu, Fe, Mn, or Co based oxides.¹⁰ To attain an optimal performance of oxygen carriers in CLC, special attention should be paid to side reactions, mainly involving the deposition of carbon from carbonaceous fuel and the evolution of sulfur species in gas fuel. Otherwise, several disadvantages would be caused from these side reactions. First, carbon deposition causes potentially the deactivation of oxygen carriers in the FR. When the carbon deposits on the oxygen carrier are transported from the FR back to the AR, CO₂ will be generated there thus causing a reduced CO₂ capture efficiency of the CLC system. Second, gas sulfur components in the syngas could possibly react with oxygen carriers and form various sulfur compounds that might be poisonous to oxygen carriers. Therefore, it is essential to understand the pathways of carbon deposition and sulfur evolution in CLC so as to eliminate the negative effects of these side reactions.

Carbon deposition is a complex phenomenon which is believed to be influenced by several factors, such as pressure, temperature, availability of lattice oxygen in the oxygen carriers, contents of H₂O(g) and CO₂ in the fuel gas, and so forth. Different measures have been investigated to inhibit the generation of solid carbon species, such as injection into the FR of a certain amount of steam, CO₂, and so on.^{11–13} The evolution of gas sulfur components was previously studied via thermodynamic analysis,^{14,15} with the predominant sulfur species in gas and solid phases predicted. It was also postulated that

besides oxygen carriers, the steam and CO₂ might also be oxidizers to convert the fuel sulfur component (H₂S) to SO₂ and other gas sulfur species (such as S₂(g) and COS). Jerndal et al.¹⁴ also analyzed the different amounts of sulfur in gas phase needed to form various sulfides or sulfates for different metal oxides. Nevertheless, research on carbon deposition and sulfur evolution in CLC is still very limited. There exist many unknowns associated with the formation of carbon deposition and the evolution of sulfur components in an FR; thus, further investigations are needed to understand both phenomena better.

As we know, coal is much more abundant than other fossil fuels and, also, more CO₂ is generated from coal utilization. It would be highly advantageous and meaningful if the gas fuel derived from coal is adopted for CLC. The feasibility of integrating coal gasification and CLC with lower energy penalties in power generation has been validated.⁹ Simulations performed by Anheden and Svedberg¹⁶ and Jin and Ishida¹⁷ indicated that CLC integrated with coal gasification had the potential to achieve a higher efficiency than a similar combined cycle using conventional CO₂ capture technology. Therefore, the syngas derived from coal gasification will be considered as the fuel gas in CLC simulation in this study. In fact, the gas components in syngas generated from coal gasification varied greatly.¹⁸ The variation range was reported for H₂ 25–30%, CO 30–60%, CO₂ 5–15%, H₂O 2–30%, H₂S 0.2–1%, and N₂ 0.2–1%. Nevertheless, in previous studies, the syngas, simply simulated as 50% CO and 50% H₂ in their volumetric fraction, was mostly adopted as the fuel for CLC simulation and experiment investigations.^{8,19} Jin and Ishida¹⁷ even used H₂, CO, H₂O(g), CO₂, and Ar to represent the syngas in their experimental study on CLC. But none of thermodynamic simulations on CLC have been conducted with a complex syngas composition as that of the fuel. Furthermore, the effect of different fuel gas compositions, particularly the occurrence of H₂O(g), CO₂, and H₂S in syngas, on the formation of carbon deposits and sulfur evolution has never been systematically studied before. It is now worthy to perform a comprehensive thermodynamic simulation with a complicated CLC system to investigate the two phenomena.

In this study, the syngas containing a mixture of gas components (CO, H₂, H₂O(g), CO₂, H₂S, N₂) was considered as a fuel in CLC for thermodynamic simulation using the HSC-Chemistry software 4.0. The reduction reactions of oxygen carriers with syngas in an FR were investigated considering five metal oxides (NiO, CuO, Fe₂O₃, Mn₂O₄, CoO). The influence of pressure, temperature, and amount of oxygen carrier was briefly investigated and followed by a detail analysis of the effect of the fuel gas composition on carbon deposition. Particularly, the occurrence of H₂O(g), CO₂, and H₂S in syngas on carbon deposition was iterated. A sensitivity analysis of the effect of these factors on carbon deposition was performed to quantita-

(3) Ishida, M.; Jin, H. A novel chemical-looping combustor without NOx formation. *Ind. Eng. Chem. Res.* **1996**, *35* (7), 2469–2472.

(4) Richter, H. J.; Knoche, K. F. *Reversibility of Combustion Processes*; ACS Symposium Series 235; American Chemical Society: Washington, DC, 1983.

(5) Jin, H.; Okamoto, T.; Ishida, M. Development of a novel chemical-looping combustion: Synthesis of a solid looping material of NiO/NiAl₂O₄. *Ind. Eng. Chem. Res.* **1999**, *38* (1), 126–132.

(6) Adánez, J.; Gayán, P.; Celaya, J.; De Diego, L. F.; García-Labiano, F.; Abad, A. Chemical looping combustion in a 10 kW prototype using a CuO/Al₂O₃ oxygen carrier: Effect of operating conditions on methane combustion. *Ind. Eng. Chem. Res.* **2006**, *45* (17), 6075–6080.

(7) Kronberger, B. Modelling analysis of fluidised bed reactor systems for chemical looping combustion. Ph.D. Thesis, Vienna University of Technology, Austria, 2005.

(8) Abad, A.; García-Labiano, F.; de Diego, L. F.; Gayán, P.; Adánez, J. Reduction kinetics of Cu-, Ni-, and Fe-based oxygen carriers using syngas (CO+H₂) for chemical-looping combustion. *Energy Fuels* **2007**, *21* (4), 1854–1858.

(9) García-Labiano, F.; Adánez, J.; de Diego, L. F.; Gayán, P.; Abad, A. Effect of pressure on the behavior of copper-, iron-, and nickel-based oxygen carriers for chemical-looping combustion. *Energy Fuels* **2006**, *20* (1), 26–33.

(10) Mattisson, T.; Lyngfelt, A. Applications of chemical-looping combustion with capture of CO₂. Presented at the Second Nordic Minisymposium on CO₂ capture and storage, Goteborg, Sweden, 2001.

(11) Cho, P.; Mattisson, T.; Lyngfelt, A. Carbon formation on nickel and iron oxide-containing oxygen carriers for chemical-looping combustion. *Ind. Eng. Chem. Res.* **2005**, *44* (4), 668–676.

(12) Ishida, M.; Jin, H.; Okamoto, T. Kinetic behavior of solid particle in chemical-looping combustion: Suppressing carbon deposition in reduction. *Energy Fuels* **1998**, *12* (2), 223–229.

(13) Ryu, H. J.; Lim, N. Y.; Bae, D. H.; Jin, G. T. Carbon deposition characteristics and regenerative ability of oxygen carrier particles for chemical-looping combustion. *Korean J. Chem. Eng.* **2003**, *20* (1), 157–162.

(14) Jerndal, E.; Mattisson, T.; Lyngfelt, A. Thermal analysis of chemical-looping combustion. *Chem. Eng. Res. Des.* **2006**, *84* (9 A), 795–806.

(15) Mattisson, T.; Johansson, M.; Lyngfelt, A. The use of NiO as an oxygen carrier in chemical-looping combustion. *Fuel* **2006**, *85* (5–6), 736–747.

(16) Anheden, M.; Svedberg, G. Chemical-looping combustion in combination with integrated coal gasification—a way to avoid CO₂ emission from coal fired power plants without a significant decrease in net power efficiency. *Proceedings of the 31st Intersociety Energy Conversion Engineering Conference*, Washington, DC, 1996; IEEE: Piscataway, NJ, 1996.

(17) Jin, H.; Ishida, M. A new type of coal gas fueled chemical-looping combustion. *Fuel* **2004**, *83* (17–18), 2411–2417.

(18) Gupta, P. Regenerable metal oxide composite particles and their use in novel chemical processes. Ph.D. Thesis, The Ohio State University, Columbus, OH, U.S.A., 2006.

(19) Johansson, E.; Mattisson, T.; Lyngfelt, A.; Thunman, H. Combustion of syngas and natural gas in a 300 W chemical-looping combustor. *Chem. Eng. Res. Des.* **2006**, *84* (9 A), 819–827.

Table 1. Composition of Syngas (vol %)

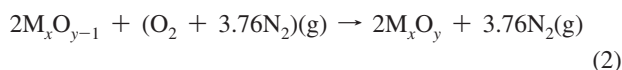
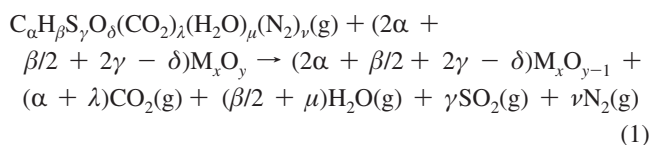
H ₂	CO	CO ₂	H ₂ O(g) ^a	H ₂ S	N ₂
25	35	10	20	3	balance

^a g: denotes the component in its gas phase.

tively evaluate their different influencing degrees. Furthermore, the effects of different factors (temperature, pressure, air excess number) and the occurrences of H₂O(g) and CO₂ in syngas on sulfur species evolution were also clarified. Finally, the predominant carbon and sulfur species in a wide temperature range were both thermodynamically predicted. This study provides much essential information for a better understanding of carbon deposition and sulfur evaluation occurring in the CLC process.

2. Method and Calculation Procedure

2.1. Design of Reaction System. The representative syngas composition used in this simulation is listed in Table 1, and its relative atomic composition could be represented as C_αH_βS_γO_δ-(CO₂)_λ(H₂O)(N₂)_ν, where the atom numbers were determined by Table 1. The reduction reaction of oxygen carriers with syngas in the FR and the reoxidation of the reduced oxygen carriers in the AR could be depicted, respectively, as follows



According to previous literature,¹⁰ five metal oxides (NiO, CuO, Fe₂O₃, Mn₃O₄, and CoO) were selected as oxygen carriers in the CLC simulation system of this study. Generally, reduced counterparts of the selected metal oxides are in elemental form, such as NiO–Ni. However, special attention should be paid to Fe, Cu, Mn, and Co oxides because of their different oxidation states. For iron, it could have several forms such as Fe₂O₃–Fe₃O₄–FeO–Fe, but in the FR of a real CLC system, because of the low conversion rate of Fe₂O₃ to other lower valence states of Fe than to Fe₃O₄, the conversion of Fe₂O₃ to Fe₃O₄ will be the predominant path.²⁰ CuO may decompose into Cu₂O in a N₂ atmosphere around 800 °C despite its stability in the air atmosphere at the same temperature but at a low decomposition rate,²¹ so the CuO–Cu pair was considered in this study with Cu₂O just included in the system as the transition form of copper oxides (as shown in Table 2). Mn₃O₄ was selected as the Mn-bearing oxygen carrier because its higher valence forms (MnO₂ and Mn₂O₃) are not stable and decompose in air at around 500 and 820 °C,²² respectively. Thus, the Mn₃O₄–MnO pair was considered as the FR temperature of interest was mainly fixed at around 950 °C.

In addition, although metal oxides are necessary to combine with various supports (such as SiO₂, Al₂O₃, TiO₂, etc.) as oxygen

carriers for CLC application, as a first step this study investigated the reduction reaction of metal oxides alone with syngas for a better understanding of their reaction characteristics. The potential effect of supports on carbon deposition and sulfur evolution in CLC will be investigated in our future study. All the chemical species considered in this calculation system for different metal oxides are shown in Table 2, including the metal oxides pairs, common gas species, deposited carbon species, and sulfur species. Almost all the related solid phase C- and S-bearing species available in the HSC database have been included to investigate the predominant carbon species that might lead to carbon deposition and the predominant sulfur species that could influence the performance of oxygen carriers in the FR of CLC.

2.2. Determination of Oxygen Excess Number Φ . The availability of oxygen present in metal oxides is one of the most important factors to determine the full conversion of fuel in the FR. Furthermore, carbon deposition and the evolution of gas sulfur components are also closely associated with the amount of oxygen carriers supplied. The theoretic stoichiometric oxygen needed for the full conversion of syngas shown in eq 1 was $(2\alpha + \beta/2 + 2\gamma - \delta)$, and supposing the realistic oxygen contained in oxygen carriers was $Y(O)$, then the oxygen excess number Φ was defined as follows

$$\Phi = Y(O)/(2\alpha + \beta/2 + 2\gamma - \delta) \quad (3)$$

In eq 3, $\Phi < 1$ denoted that the oxidation of syngas with oxygen carriers was initiated under an oxygen-deficient condition; $\Phi > 1$ meant that the reaction was occurring in an oxygen-rich environment; and $\Phi = 1$ referred to that the oxygen supplied theoretically just met the requirement of a full conversion of fuel.

2.3. Calculation Method. The reduction reaction of various metal oxides with syngas in the FR was investigated using the HSC-Chemistry software 4.0 and based on the minimization of the total Gibbs free energy. The predominant equilibrium compositions in the FR were simulated, with focus on the carbon- and sulfur-bearing species, at various pressures (1, 10, 15, and 30 bar), temperatures (mainly 100–1400 °C for all metal oxides except for CuO at a relatively lower temperature, because of the much lower melting point of the reduced element Cu, i.e., ~1085 °C), and oxygen excess numbers Φ (including $\Phi < 1$, $\Phi = 1$, and $\Phi > 1$, respectively). It was noteworthy that the thermodynamic equilibrium analysis did not consider any kinetic constraints, such as, mixing and/or temperature gradients occurring in the real process; thus, experimental works were needed to verify the simulations. Nevertheless, the equilibrium calculation provides a useful guide for predicting major species in the system, allowing a better understanding of the complex reactions to happen in the CLC system, including those associated with carbon deposition and sulfur evolution.

In view of carbon deposition, first, a simple syngas system (containing only CO, N₂, and H₂) was considered to investigate the effect of temperature, pressure, and Φ . Then, the fuel gas composition was changed by introducing H₂O(g), CO₂, and H₂S separately into the simple system, aiming to understand their different effects on carbon deposition. Furthermore, to compare the degree of influence of these factors on carbon deposition, a sensitivity analysis was performed, and the relative linear sensitivity coefficient ω_i of carbon deposition amount m toward various factors χ_i (including temperature, pressure, Φ , the

(20) Cho, P.; Mattisson, T.; Lyngfelt, A. Defluidization conditions for a fluidized bed of iron oxide-, nickel oxide-, and manganese oxide-containing oxygen carriers for chemical-looping combustion. *Ind. Eng. Chem. Res.* **2006**, *45* (3), 968–977.

(21) Corbella, B. M.; de Diego, L.; Garcia-Labiano, F.; Adanez, J.; Palacios, J. M. Characterization and performance in a multicycle test in a fixed-bed reactor of silica-supported copper oxide as oxygen carrier for chemical-looping combustion of methane. *Energy Fuels* **2006**, *20* (1), 148–154.

(22) Johansson, M.; Mattisson, T.; Lyngfelt, A. Investigation of Mn₃O₄ with stabilized ZrO₂ for chemical-looping combustion. *Chem. Eng. Res. Des.* **2006**, *84* (9 A), 807–818.

Table 2. Species Considered in the HSC Calculation for Various Metal Oxides^a

metal oxides	NiO–Ni	Fe ₂ O ₃ –Fe ₃ O ₄	CuO–(Cu ₂ O)–Cu	Mn ₃ O ₄ –MnO	CoO–Co
common species	H ₂ (g), H ₂ O(g) CO(g), CO ₂ (g), CH ₄ (g), C(g), C ₂ (g), C ₃ (g), C ₄ (g), C ₅ (g), C, C(A), C(D) H ₂ S(g), SO ₂ (g), SO ₃ (g), COS(g), S(g), S ₂ (g), S ₃ (g), S ₄ (g), S ₅ (g), S ₆ (g), S ₇ (g), S ₈ (g), CS(g), CS ₂ (g), S N ₂ (g), NO(g), NO ₂ (g), NO ₃ (g), N ₂ O(g), N ₂ O ₂ (g), N ₂ O ₃ (g), N ₂ O ₄ (g), N ₂ O ₅ (g)				
deposited carbon species	Ni ₃ C	Fe ₃ C Fe ₃ C(B)		MnC ₂ , Mn ₃ C Mn ₇ C ₃ Mn ₁₅ C ₄ Mn ₂₃ C ₆	Co ₂ C
	NiCO ₃	FeCO ₃	CuCO ₃ Cu ₂ (OH) ₂ CO ₃ Cu ₃ (OH) ₂ (CO ₃) ₂	MnCO ₃	CoCO ₃
deposited sulfur species	NiS _{0.84} NiS, NiS(A) Ni ₃ S ₂ , Ni ₃ S ₄	Fe _{0.877} S FeS, FeS ₂ FeS ₂ (M) Fe ₂ S ₃ , Fe ₇ S ₈	CuS Cu ₂ S	MnS MnS ₂	CoS _{0.89} , CoS CoS _{1.333} CoS ₂ , Co ₃ S ₄ Co ₉ S ₈
	NiSO ₄ NiSO ₄ ·H ₂ O NiSO ₄ ·4H ₂ O NiSO ₄ ·6H ₂ O NiSO ₄ ·7H ₂ O	FeSO ₄ Fe ₂ (SO ₄) ₃ FeSO ₄ ·H ₂ O FeSO ₄ ·4H ₂ O FeSO ₄ ·7H ₂ O	CuSO ₄ Cu ₂ SO ₄ CuSO ₄ ·H ₂ O CuSO ₄ ·3H ₂ O CuSO ₄ ·4H ₂ O CuO·CuSO ₄	MnSO ₄ MnSO ₄ ·H ₂ O MnSO ₄ ·4H ₂ O MnSO ₄ ·5H ₂ O MnSO ₄ ·7H ₂ O	CoSO ₄ CoSO ₄ ·6H ₂ O CoSO ₄ ·7H ₂ O

^a g is the gaseous state; C(A) and C(D) are amorphous and diamond carbon, respectively; Fe₃C(B) is β -iron carbide and FeS₂(M) is marcasite; NiS(A) is α -nickel sulfide.

content of H₂O(g), CO₂, and H₂S in the syngas) was calculated by the finite difference method.²³

$$\omega_i = \frac{\Delta m/m}{\Delta \chi_i / \chi_i} \quad (4)$$

where i denotes the various factors mentioned above. The parameters of these factors adopted as the base case were the FR temperature 600 °C (the same as Jin et al. used¹²), pressure 1 bar, $\Phi = 0.5$, and the volume of H₂O(g) 20%, of CO₂ 10%, and of H₂S 3%, respectively. After five calculations were performed for each factor changing the factor value from the base case while keeping other parameters constant, it was found that the results of the sensitivity analysis showed the same tendency for the same factor. Therefore, only one representative case was reported. Finally, the distribution of various carbon-bearing species was analyzed considering the complicated syngas system containing all the gas species as shown in Table 1, under different pressures, FR temperatures, and oxygen excess numbers Φ .

Furthermore, the sulfur evolution in CLC was simulated first in a simple system of syngas (CO, N₂, H₂, and H₂S). After that, H₂O(g) and CO₂ were introduced separately into the system, and the influence of their presence on sulfur distribution was evaluated. Finally, various sulfur species were predicted in the FR of the CLC system with the complete syngas as fuel and under different conditions as shown in Table 1.

3. Results and Discussion

3.1. Carbon Deposition. *3.1.1. Effect of Various Factors on Carbon Deposition.* The occurrence of carbon deposition in the FR was predicted under various conditions, and the results are depicted in Figure 2. The conditions for forming carbon deposits (i.e., various carbon species in the solid phase) in a simple syngas (CO, N₂, H₂) system are summarized in Figure 2a, with varying temperature, pressure, and Φ . The three solid

lines denote the equilibrium boundary of free carbon deposition at three pressures (1, 10, and 30 bar) and at various oxygen excess numbers Φ (0–0.9) and FR temperatures (400–1300 °C). The area below each boundary indicates the carbon deposition region while the area above denotes no solid carbon formation under the related condition. At the beginning, it was found that at a fixed pressure and Φ the area of carbon deposition decreased with FR temperature increase. Meanwhile, at a fixed FR temperature and atmospheric pressure, a larger Φ (i.e., more oxygen carrier) was needed to reach the area of “no carbon deposition”. Also, the pressurized condition caused the area of carbon deposition to increase. Overall, high temperature, low pressure, and sufficient oxygen carriers were beneficial to reduce the carbon deposition. This simulation result was similar to that of Jerndal et al.,¹⁴ though the fuel used in this study was syngas instead of methane.

Furthermore, the effect of H₂O(g) content in syngas on carbon deposition was investigated by introducing steam at different concentrations into the simple syngas as the fuel of CLC. The simulated results are presented in Figure 2b. First, it was found that at a fixed FR temperature and Φ , the area of carbon deposition decreased with H₂O(g) content in the syngas. A higher FR temperature produced less deposited carbon on the oxygen carrier, similar to the findings in Figure 2a. In terms of the inhibition mechanism of carbon deposition with the addition of H₂O(g), Jerndal et al.¹⁴ reported that the H₂O(g) acted as the additional lattice oxygen source, similar to the oxygen provided by the oxygen carrier, to enhance the conversion of carbon deposit to CO₂ while Ishida et al.¹² believed that the H₂O(g) addition initiated the shifting reaction of CO in syngas and thus reduced the conversion of CO to carbon via the Boudouard reaction. Similarly, the CO₂ and H₂S were introduced separately into the system (data not shown here). CO₂ behaved quite similarly as H₂O(g) in inhibiting carbon deposition through possibly different mechanisms while the addition of H₂S led to more solid carbon deposition. Nevertheless, further research is needed to obtain a better understanding of the different effects of steam, CO₂, and H₂S on carbon deposition. In the complicated

(23) Rabitz, H.; Kramer, M.; Dacol, D. Sensitivity analysis in chemical kinetics. *Annu. Rev. Phys. Chem.* **1983**, *34*, 419–461.

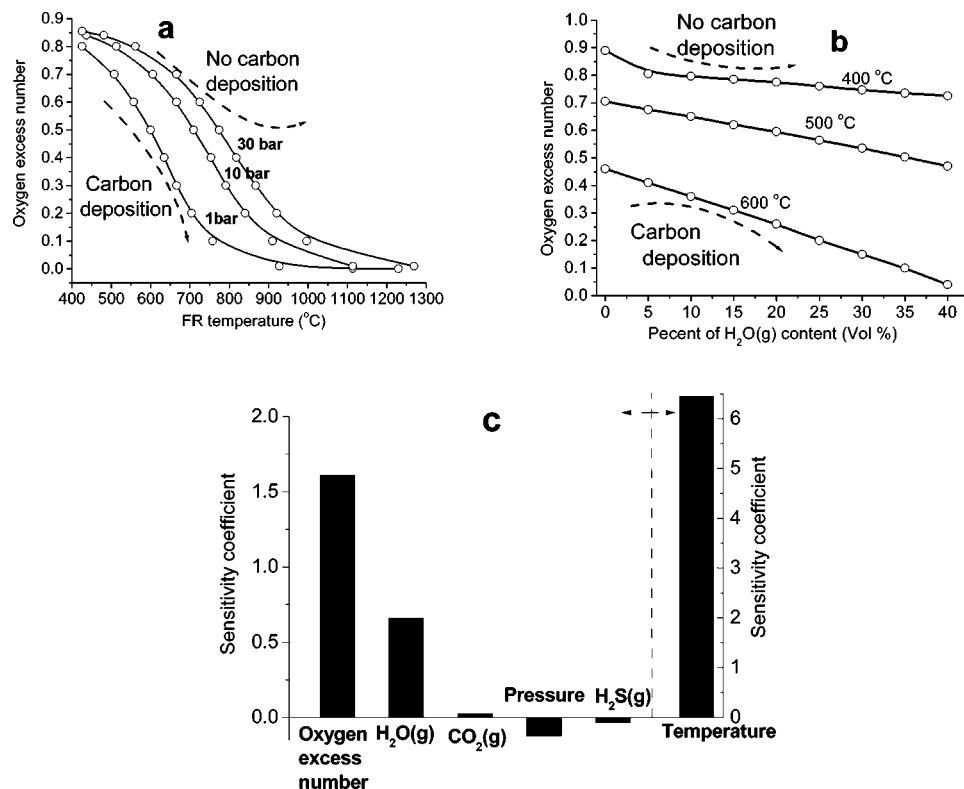


Figure 2. Effects of different factors on carbon deposition: (a) effect of temperature, pressure, and oxygen excess number Φ in a simple syngas system; (b) effect of H₂O(g) content on carbon deposition; and (c) sensitivity coefficient of various factors on carbon deposition.

syngas system (see Table 1), the influence of changing temperature and pressure demonstrated almost the same tendency of effects as those observed in the simple system (Figure 2a). The only difference found was that, at the same FR temperature and pressure, the area of free carbon deposition for the complicated syngas system was far enlarged compared to that for the simple system, most likely because of the synergistic effect of H₂O(g), H₂S, and CO₂ on carbon deposition.

A sensitivity analysis was conducted to understand the different extents of the considered factors on carbon deposition. The sensitivity coefficient values of various factors on carbon deposition are shown in Figure 2c, which were generated by changing the parameters from the base case to temperature 500 °C, pressure 10 bar, and $\Phi = 0.6$ and the volume of H₂O(g) to 10%, of CO₂ to 20%, and of H₂S to 0%, respectively. First, the sensitivity values of temperature, Φ , and the contents of H₂O(g) and CO₂ toward the variation of carbon deposition were positive, which meant that increase of these parameters would eliminate carbon deposition. Nevertheless, the sensitivity values of pressure and content of H₂S were negative, which implied that increase of these parameters would cause more deposited carbon, similar to the finding reported by Jerndal et al.¹⁴ Furthermore, the influence of temperature on eliminating carbon deposition was the most significant with the sensitivity coefficient over 6 as indicated by the right-side Y-axis. Following it, Φ and the content of steam showed their sensitivity coefficients respectively at ~ 1.5 and 0.5, as indicated by the left-side Y-axis. The content of CO₂ demonstrated the minimal eliminating effect on carbon deposition. On the contrary, the pressure showed a higher potential than the content of H₂S in causing carbon deposition. Furthermore, the effect of H₂O(g) on the inhibition of carbon deposition was greater than that of CO₂ (Figure 2c), which was the same as the previous finding.¹² This indicated that, at the same reaction condition, the addition of H₂O(g) was more effective than that of CO₂ to inhibit solid carbon formation.

3.1.2. Predominant Carbon-Bearing Species for the Studied Metal Oxides. The equilibrium distributions of various C-bearing species in CLC at different pressures (1 bar, "solid line"; 15 bar, "dashed line") and fixed Φ (0.5) for different metal oxides (NiO, Fe₂O₃, CuO, Mn₃O₄, and CoO) are shown in Figure 3a,c,d,e,f, respectively. In addition, the predominant C-bearing species for NiO were simulated at different oxygen excess numbers ($\Phi = 0.8$ and 1.2) at 1 bar, and the result is given in Figure 3b. The discussions on Figure 3 are given below.

(i) *Effect of Temperature.* In Figure 3a,d,e,f with temperature increasing from 100 to 1400 °C as well as in Figure 3c for CuO with the FR temperature to 1085 °C, CO₂ was found as the predominant carbon species in the whole temperature range for almost all the metal oxides studied. The percentages of CO became significant from 600 °C onward for the four metal oxides, except for Mn₃O₄. Various carbon deposits (mostly carbon and metal-carbonates) were found generally at low temperature while at high temperature (>1000 °C) only CO₂ and CO are thermodynamically stable carbon species. It is noteworthy that, for Mn₃O₄, the deposited carbon species were mainly MnCO₃ and MnC₂, different from other metal oxides.

In Figure 3, CH₄ was always generated and mainly occurred at low temperature (below 700 °C) for most of the metal oxides studied except for Mn₃O₄. This basically agreed with the previous findings²⁴ where a laboratory fluidized bed reactor was used to test different oxygen carriers. Although there was no CH₄ present in the syngas supplied (50% H₂ and 50% CO), CH₄ was found to form through the methanation reaction of CO and H₂, especially at low FR temperature (generally below 600 °C). Furthermore, in this

(24) Mattisson, T.; Johansson, M.; Lyngfelt, A. CO₂ capture from coal combustion using chemical-looping combustion - reactivity investigation of Fe, Ni and Mn based oxygen carriers using syngas. Presented at the 2006 Clearwater Coal Conference, Clearwater, FL, U.S.A., 2006.

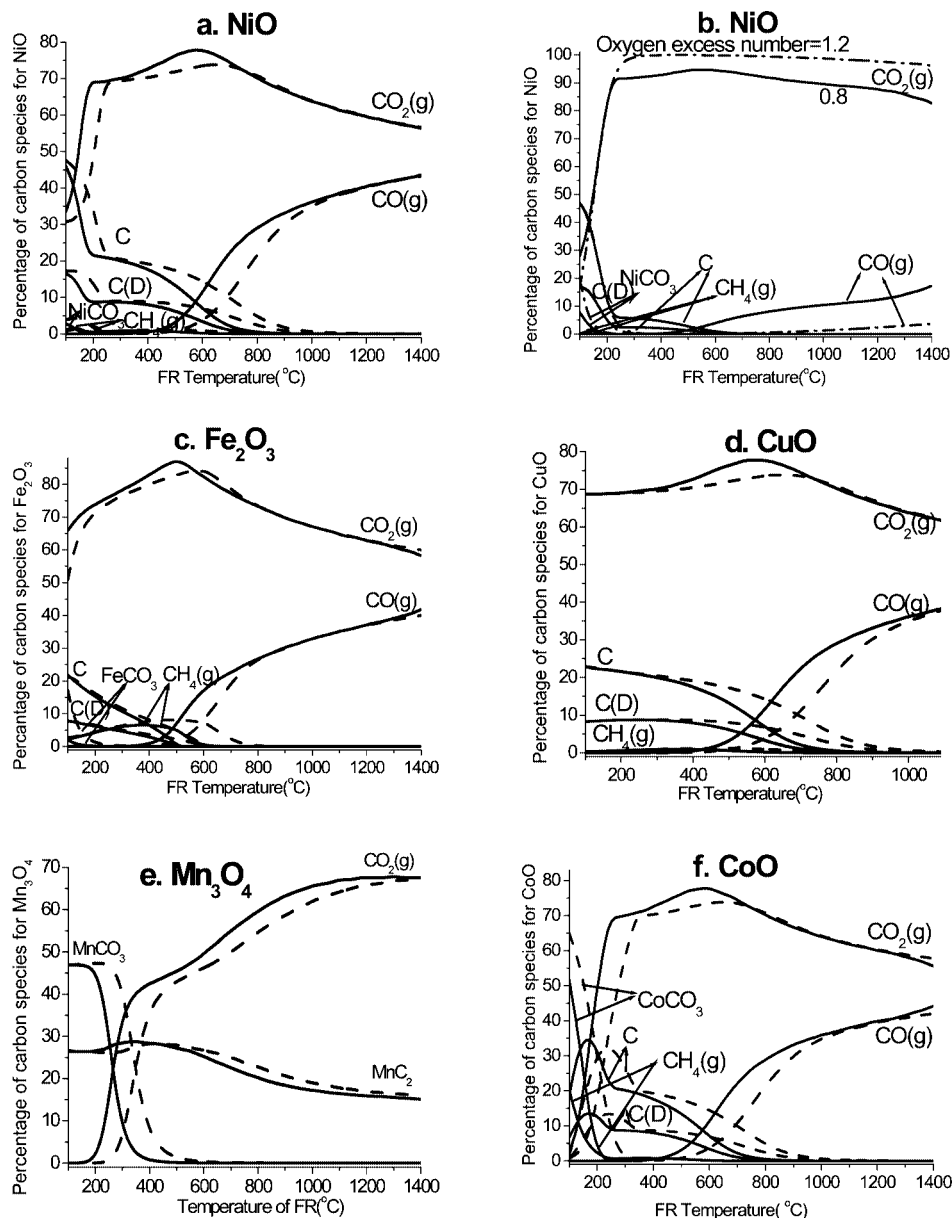


Figure 3. Equilibrium distribution of various carbon species for different metal oxides, (a, b) NiO, (c) Fe₂O₃, (d) CuO, (e) Mn₃O₄, and (f) CoO. The simulated conditions are oxygen excess number $\Phi = 0.5$, pressure $P = 1$ bar (solid line), $\Phi = 0.5$, $P = 15$ bar (dash line) for parts a, c, d, e, and f, respectively, but for part b, $\Phi = 0.8$, $P = 1$ bar (solid line) and $\Phi = 1.2$, $P = 1$ bar (dashed-dotted line) were used.

study it was found that the percentages of CH₄ diminished with increasing pressure and Φ .

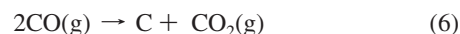
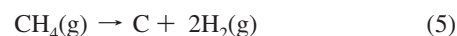
(ii) *Effect of Pressure.* When pressure was increased from 1 to 15 bar for various metal oxides studied, the equilibrium percentages of CO₂ and CO somewhat declined at the studied temperature range; thus, the percentages of various solid carbon species increased. Especially at low FR temperature (mainly at 100–600 °C), the percentages of elemental carbons and relative carbonates of the studied metal oxides were strikingly increased.

(iii) *Effect of Φ .* In Figure 3b, with Φ changing from 0.8 to 1.2, the CO₂ equilibrium percentage increased obviously to nearly 100% from a very low temperature (around 200 °C), corresponding to a decrease of CO equilibrium percentage. The percentages of various deposited carbon species declined to a large degree from $\Phi = 0.5$ (see Figure 3a) to $\Phi = 0.8$ and 1.2 (see Figure 3b), most likely because of the enhanced conversion of elemental carbon to CO₂ with more oxygen supplied.

(iv) *Predominant C-Bearing Species.* In Figure 3, the deposited carbon species were mainly elemental carbons and

their carbonates for NiO, Fe₂O₃, and CoO while for CuO only elemental carbon was predicted as its main carbon deposits. Different to others, the deposited carbon species for Mn₃O₄ were MnCO₃ and MnC₂.

3.1.3. *Carbon Deposition Pathway in CLC with Syngas.* As reported by different researchers,^{11–13} there are two possible routes to form carbon deposition in CLC: catalytic methane decomposition (eq 5) and the Boudouard reaction (eq 6).



Both reactions are known to be slow, but with the presence of catalysts such as Ni, these reactions can be readily catalyzed to occur. It was found that at high reaction temperature (above 617 °C), the deposited carbon mainly arose from the decomposition of CH₄, that is, eq 5, while at low reaction temperature (397 °C), the Boudouard reaction, that is, eq 6, was favored.

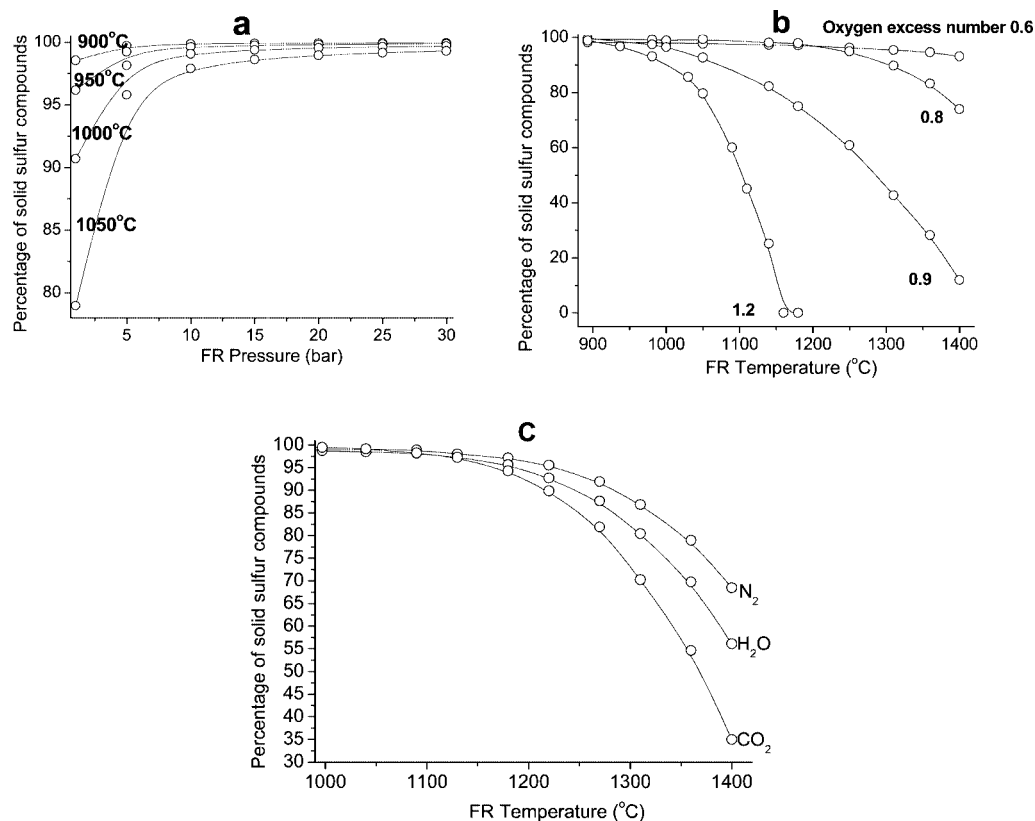


Figure 4. Effects of different factors on the percentage of solid sulfur compounds: (a) effect of pressure and temperature in the simple syngas without H₂O(g) and CO₂, pressure 1 bar, and oxygen excess number $\Phi = 1.2$; (b) effect of oxygen excess number Φ in the simple syngas, pressure 1 bar; and (c) effect of H₂O(g) and CO₂, pressure 1 bar, oxygen excess number $\Phi = 0.8$, and 30% of H₂O(g), CO₂, or N₂ was separately introduced into the simple syngas.

According to the thermodynamic simulation results (Figure 3), the formation of CH₄ was inevitable, especially at low FR temperature (below 600 °C). Because methane decomposition occurs at relatively high temperature (>617 °C) and only trace amounts of methane formed at relatively low temperature (<600 °C), it was unlikely for carbon deposition to happen via catalytic methane decomposition. Therefore, the Boudouard reaction, that is, eq 6, was most possibly the main pathway of carbon deposition in CLC of syngas.

3.2. Evolution of Sulfur in CLC of Syngas. **3.2.1. Effect of Various Factors on Sulfur Species Distribution.** The formation of solid sulfur species and their potential depositions on oxygen carriers are also a big concern to CLC. The effects of various factors (including temperature, pressure, and Φ) on the percentage of solid sulfur compounds in CLC were investigated at first with the simple syngas (CO, N₂, H₂, and H₂S) as the fuel and NiO as oxygen carrier. Following that, 30% H₂O(g) and CO₂ each were introduced separately into the syngas, and the effects of their occurrences on solid sulfur percentages were also explored. The simulated results are shown in Figure 4. Concerning the effect of temperature and pressure, it was found that the percentage of solid sulfur compounds obviously increased with pressure rising from 1 to 10 bar while it remained almost unchanged with a further increase of pressure to 30 bar. Furthermore, with the FR temperature increasing from 900 to 1050 °C and at a FR pressure of 1–10 bar, the percentage of solid sulfur compounds correspondingly decreased.

The effect of oxygen excess number Φ on the percentage of solid sulfur compounds is shown in Figure 4b. With Φ increasing, the percentage of solid sulfur compounds sharply decreased, which implied that more solid sulfur compounds were

converted into gas sulfur species. Particularly, all these changes happened at FR temperature above 1000 °C.

Figure 4c shows the effects of introducing H₂O(g), CO₂, or N₂ (taken as the reference case) on the percentage of solid sulfur compounds. In this case, the simulated condition was set as $\Phi = 0.8$, pressure 1 bar. At 1150–1400 °C of FR temperature, when 30% of CO₂, H₂O(g), or N₂ were separately introduced into the simple syngas system, the percentage of solid sulfur compounds steeply declined with FR temperature. The effect of CO₂ was the most significant, followed by H₂O(g) and N₂. The change caused by introducing N₂ (inert gas) into the system (as a reference case) reflected actually the sole effect of increasing temperature on the percentage of solid sulfur in the system. It implied that with the same amount of CO₂ or H₂O(g) included in the simple syngas, more solid sulfur was converted into gas species, most likely because of chemical interactions. Furthermore, in the studied condition ($\Phi = 0.8$, 1150–1400 °C, 1 bar), SO₂ will be the predominant gas species (to be confirmed with thermodynamic simulations shown in the subsequent text). This indicated that the oxidation capacity of CO₂ in converting solid sulfur or H₂S into SO₂ was greater than that of H₂O(g), especially at the studied condition. This result was consistent with the earlier reports which indicated CO₂ and H₂O(g) were possible oxidizers to convert H₂S to mainly SO₂,^{14,15} especially under oxygen-deficient conditions. In addition, similar conclusions could also be reached from simulations with other metal oxides besides NiO, though the details (not shown here) somewhat differed. Further investigations are needed to understand the mechanisms related to the oxidation effects of CO₂ and H₂O(g) in syngas, as observed from this simulation.

3.2.2. Predominant Sulfur Compounds. The equilibrium distributions of various sulfur species at atmospheric pressure

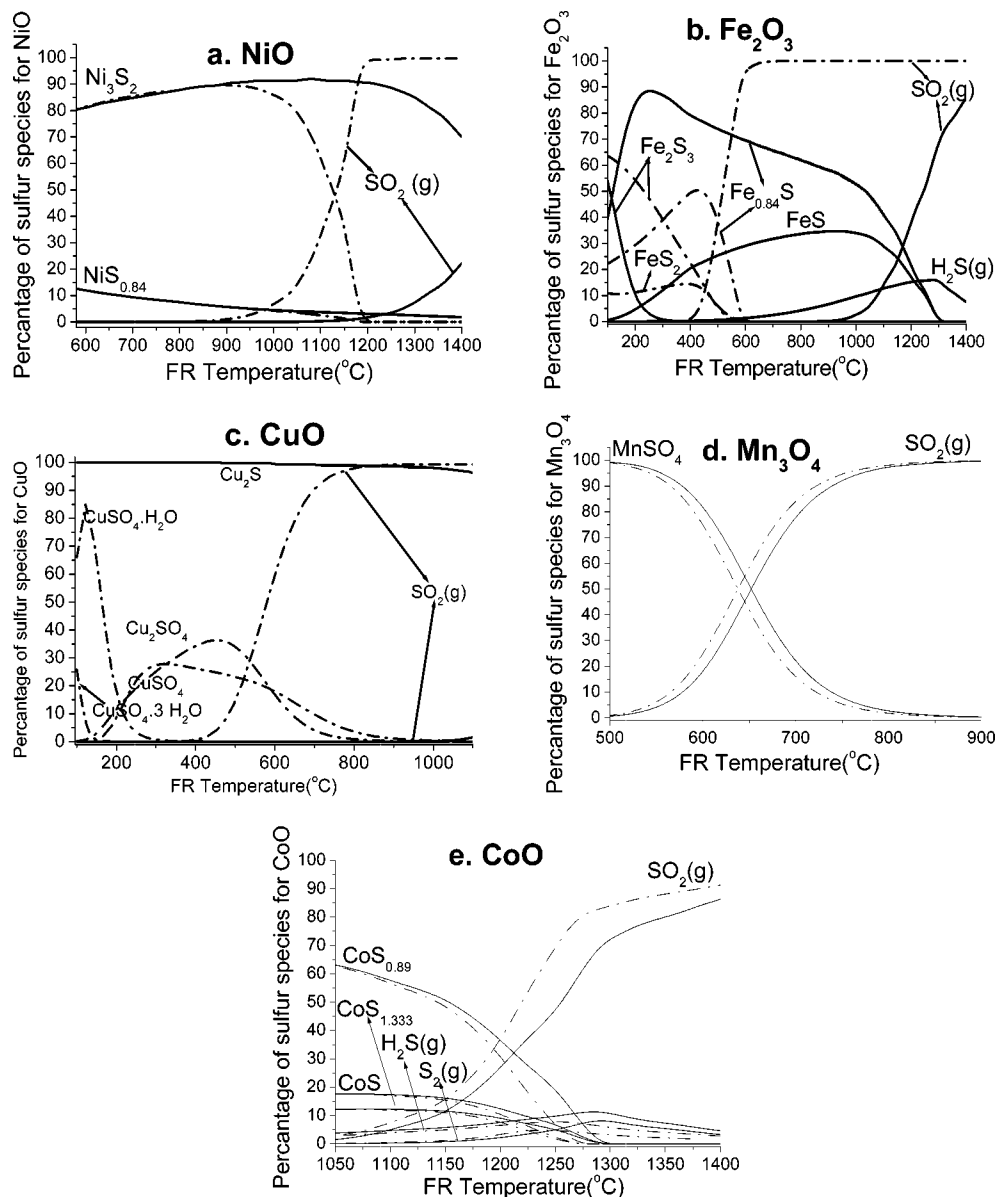


Figure 5. Equilibrium distribution of various sulfur species for different metal oxides, (a) NiO, (b) Fe₂O₃, (c) CuO, (d) Mn₃O₄, and (e) CoO, respectively. The simulated condition is $\Phi = 0.8$ (solid line) and 1.2 (dashed-dotted line), pressure 1 bar.

and $\Phi = 0.8$ and 1.2, respectively, for different metal oxides, NiO, Fe₂O₃, CuO, Mn₃O₄, and CoO, are shown in Figure 5. From these figures, two main findings could be attained.

(i) *Effect of Oxygen Excess Number Φ and Temperature.* The oxygen excess number Φ influenced the evolution of the sulfur species greatly. With Φ increasing from 0.8 to 1.2, the percentages of sulfur species with low valences (such as H₂S and sulfides) were decreased, accompanied by the increase of SO₂ percentage at high temperature. H₂S was only found at $\Phi = 0.8$ for Fe₂O₃ and CoO as oxygen carriers. In contrast, SO₂ was thermodynamically not stable at $\Phi = 0.8$ for NiO and CuO while it was mainly produced at oxidizing conditions ($\Phi = 1.2$). It indicated that more sulfur deposition might form at oxygen-deficient conditions. This agreed with the finding obtained from Figure 4b.

The equilibrium percentage of SO₂ was also increased with the FR temperature, similar to the conclusion of Jerndal et al.¹⁴ At whatever oxygen excess number Φ , the deposited solid sulfur species were always present at relatively low temperature. Furthermore, the temperature of nearly full conversion of sulfur (mostly H₂S and sulfides) into SO₂ in the FR was above 1100 °C for NiO (at $\Phi = 1.2$), Fe₂O₃ (at $\Phi = 0.8$), and CoO (both

$\Phi = 0.8$ and 1.2), which was far bigger than that for Fe₂O₃ (at $\Phi = 1.2$), CuO (at $\Phi = 1.2$), and Mn₃O₄. It implied that more gas sulfur species (correspondingly less sulfur solid deposits) were possibly generated for the latter three cases at the real FR temperature (800–1000 °C) in the CLC system.

(ii) *Predominant Sulfur Compounds Distribution.* The solid sulfur species with the largest percentages, which meant the most possible sulfur compounds deposited on oxygen carriers in CLC, at both oxidizing and reducing conditions. For CuO, at $\Phi < 1$, the sulfide (Cu₂S) was the most thermodynamically possible solid sulfur compound while for $\Phi > 1$ various solid copper sulfates dominated at low temperature.

4. Conclusions

A full conversion of gas fuel in the FR is crucial to enhance the CO₂ separation efficiency of the CLC system. Side reactions,

including carbon deposition and sulfur evaluation from trace H_2S contained in the gas fuel, are detrimental to the performance of oxygen carriers and thus inhibit the conversion of gas fuel. These side reactions were studied through thermodynamic simulation in considering five metal oxides (i.e., NiO , CuO , Fe_2O_3 , Mn_3O_4 , and CoO) as the oxygen carriers and syngas as the fuel. The effects of various factors (including temperature, pressure, oxygen excess number Φ , and the contents of $\text{H}_2\text{O}(\text{g})$ and CO_2 in the syngas) on these side reactions were considered. On the basis of the simulation results, the following conclusions were reached.

(i) Carbon deposition and the evolution of sulfur in CLC were influenced largely by various factors. At whatever conditions considered, the pressurized condition led to more solid carbon and sulfur species deposited on oxygen carriers. A higher FR temperature favorably enhanced full conversion of syngas as evidenced by the significant decrease of carbon deposits and the conversion of most sulfur compounds into SO_2 at high temperature. A bigger Φ decreased the tendency of carbon deposition and led to more gas sulfur species formed, mainly SO_2 .

(ii) The effects of $\text{H}_2\text{O}(\text{g})$ and CO_2 in the syngas on both side reactions were further clarified. Through sensitivity analysis of various influencing factors on carbon deposition, the increase of H_2O and CO_2 contents in syngas could inhibit carbon

formation, and the inhibition degree of $\text{H}_2\text{O}(\text{g})$ was greater than that of CO_2 while the increase of the H_2S fraction in syngas led to more carbon deposition. In terms of the effect of $\text{H}_2\text{O}(\text{g})$ and CO_2 in syngas on the conversion of sulfur compounds into SO_2 , the oxidation effect of CO_2 was found to be stronger than that of $\text{H}_2\text{O}(\text{g})$, especially at oxygen-deficient conditions.

(iii) The carbon and sulfur compounds that potentially deposit on the oxygen carrier were speciated. At low FR temperature and oxygen-deficient conditions, the main carbon deposited species for NiO , Fe_2O_3 , CuO , and CoO were C and C(D), while for Mn_3O_4 , MnCO_3 , and MnC_2 were mainly deposited carbon species. Meanwhile, the most possible solid sulfur compounds deposited on oxygen carriers were Ni_3S_2 , $\text{Fe}_{0.84}\text{S}$, MnSO_4 , and $\text{CoS}_{0.89}$ for NiO , Fe_2O_3 , Mn_3O_4 , and CoO . But for CuO , under oxygen-deficient conditions, that is, $\Phi < 1$, the sulfur deposited compound was Cu_2S ; in contrast to this, at $\Phi > 1$, $\text{CuSO}_4 \cdot \text{H}_2\text{O}$ was formed at 100–200 °C, and at 200–500 °C, the deposited sulfur compounds were mainly CuSO_4 and Cu_2SO_4 .

Acknowledgment. This work is part of the project “Co-control of Pollutants during Solid Fuel Utilization”, supported by the Programme of Introducing Talents of Discipline to Universities (project B06019), China; it is also supported by the project of National Natural Science Foundation of China (No. 50676038).

EF7005673